Research Square

Preprints are preliminary reports that have not undergone peer review.
They should not be considered conclusive, used to inform clinical practice,
or referenced by the media as validated information.

Replication, Parasite Control, and Energy Metabolism in Autocatalytic RNA Systems: A Minimal Computational Model

Bernard Conrad

bernard.conrad@genesupport.ch

Genesupport

Christian Iseli

École Polytechnique Fédérale de Lausanne

Magnus Pirovino

OPIRO Consulting Ltd.

Research Article

Keywords: RNA world, Autocatalytic ribozyme networks, Molecular parasitism, Allosteric regulation, ATP/ADP energy cycle, Origin of life

Posted Date: November 10th, 2026

DOI: https://doi.org/10.21203/rs.3.rs-11409330/v1

License: This work is licensed under a Creative Commons Attribution 4.0 International License.
Read Full License

Additional Declarations: No competing interests reported.

Replication, Parasite Control, and Energy Metabolism in Autocatalytic RNA Systems: A Minimal Computational Model

Bernard Conrad[1*], ORCID ID 0000-0002-3662-9041, Christian Iseli[2], ORCID ID 0000-0002-2296-2863, Magnus Pirovino[3]

[1]Genesupport, Rte de la Corniche 11, 1066 Epalinges, Switzerland

[2]Bioinformatics Competence Center, EPFL and Unil, Lausanne, Switzerland

[3]OPIRO Consulting Ltd., Triesen, Principality of Liechtenstein

*Corresponding author

E-Mail: bernard.conrad@genesupport.ch

Abstract

Self-sustained proto-Darwinian replication in an RNA world requires mechanisms to control molecular parasitism while sustaining the energetic demands of replication. How minimal RNA systems could coordinate replication, energy metabolism, and regulation remains an open question in origin-of-life research. Here, we develop a mathematical model of an autocatalytic ribozyme network integrating template-directed replication, an ATP/ADP energy cycle, and ATP-dependent allosteric regulation. In the absence of regulation, replication-error-derived parasites exploit the replicase and can destabilize or collapse the network. We show that allosteric interactions involving ATP-bound parasitic ribozymes and hyperparasites—parasites of parasites—can establish regulatory control and stabilize the system. Hyperparasites interact with the replicase and both ATP-bound and ATP-free parasitic ribozymes, but their sequestration of ATP imposes energetic constraints on replication. Increasing ATP turnover can alleviate these constraints, revealing a fundamental trade-off between parasite suppression and energy availability. Regulatory control can arise through two distinct mechanisms: intrinsically allostery-prone parasitic RNAs or trans-acting “allosterase” parasites that confer allosteric regulation on other RNAs. Once regulatory stability is established, catalytic ATP synthase/ATPase ribozymes can enhance ATP/ADP cycling, increasing energetic capacity and adaptability. These findings suggest a plausible evolutionary sequence in which parasite-mediated regulation precedes energetic optimization. More broadly, our model illustrates how molecular parasitism, rather than merely threatening early replicating systems, could contribute to the emergence of regulatory organization and increasingly autonomous proto-metabolic networks.

Key Words

RNA world, Autocatalytic ribozyme networks, Molecular parasitism, Allosteric regulation, ATP/ADP energy cycle, Origin of life

Introduction

Origin-of-life scenarios have traditionally been framed around two contrasting principles: the metabolism-first and replication-first hypotheses (Anet 2004; Pross 2004). The metabolism-first view proposes that self-organized reaction networks initially harnessed geochemical energy to drive organic synthesis, with prebiotic catalysis progressively giving rise to biological metabolism (Zimmermann et al. 2024). Within this framework, the architecture of ancient chemolithoautotrophic pathways, including carbon fixation through the reductive citric acid cycle, may preserve features of primordial nonenzymatic reaction networks (Morowitz 1999). Conversely, replication-first scenarios propose that the emergence of self-replicating informational polymers, particularly RNA, preceded the development of increasingly complex metabolic systems. Irrespective of their evolutionary sequence, however, the emergence of autonomous evolving systems ultimately required the functional integration of energy conversion, information replication, and mechanisms controlling molecular parasitism. How these functions could have become dynamically coupled within minimal molecular networks remains a fundamental question in origin-of-life research.

Adenosine triphosphate (ATP) occupies a central position at the interface of metabolism and heredity. In extant life, it serves as a principal energy currency while simultaneously functioning as one of the four nucleoside triphosphate substrates of RNA synthesis. ATP also participates extensively in core metabolic pathways, including those associated with ancient forms of chemolithoautotrophic metabolism based on H_2 and CO_2 (de Duve 2005; Pinna et al. 2022). Several reactions within these pathways can proceed without enzymes, supporting the hypothesis that early metabolic networks originated from geochemically driven processes (Wimmer et al. 2021). However, contemporary purine biosynthesis requires multiple ATP-dependent phosphorylation reactions, creating a potential evolutionary bootstrap problem in which ATP is required for its own synthesis (Pinna et al. 2022). This suggests that simpler phosphorylating agents may have preceded ATP in early energy metabolism. Acetyl phosphate, a conserved intermediate connecting thioester and phosphate chemistry, has been proposed as one such precursor. Its experimentally demonstrated ability to phosphorylate ADP under aqueous conditions supports a potential role in prebiotic energy transfer (Whicher et al. 2018; Pinna et al. 2022).

Additional evidence for an ancient connection between metabolism and RNA comes from the molecular architecture of coenzymes. Many coenzymes contain nucleotide-derived structural elements, particularly adenosine monophosphate moieties, and several appear to have retained essential biochemical functions since the last universal common ancestor (Kirschning 2022; Zimmermann et al. 2024). These features have motivated the hypothesis that nucleotide-containing cofactors preserve molecular signatures of early catalytic systems. Morowitz similarly proposed that the diversification of biomolecules from a restricted core of carbon-fixation reactions could have generated the molecular precursors of genetic systems through the progressive expansion of protometabolic networks (Morowitz 1999; Zimmermann et al. 2024). Such observations suggest that the emergence of RNA-based heredity and the evolution of energy metabolism may have been closely interconnected, regardless of which process arose first.

The RNA world hypothesis proposes that early evolving systems relied on RNA molecules capable of both storing genetic information and catalyzing chemical reactions (Gilbert 1986). Abiotic polymerization and subsequent recombination of RNA oligomers may have generated structurally diverse molecules, some exhibiting catalytic activities such as RNA ligation (Briones 2009). Experimental studies have demonstrated that Group I intron-derived ribozymes can assemble from shorter RNA fragments through recombination, illustrating plausible routes toward increasingly complex autocatalytic systems (Hayden 2006). Progressive functional diversification could subsequently have generated RNA polymerase ribozymes capable of template-directed replication, establishing the molecular basis for Darwinian evolution (Nghe 2025).

However, the emergence of template-directed replication would also introduce a fundamental evolutionary vulnerability: molecular parasitism. Replication errors can generate RNA variants that retain access to replication machinery while losing catalytic functions required for maintaining the network. By exploiting the replication capacity of functional ribozymes without contributing equivalent catalytic activity, such parasites can acquire a selective advantage and potentially destabilize autocatalytic systems. Consequently, sustained RNA-based evolution requires mechanisms that limit parasite proliferation while preserving the catalytic and energetic functions necessary for replication. Although spatial organization and compartmentalization provide potential solutions, molecular regulatory interactions offer an alternative route through which parasite dynamics could become integrated into the stability of autocatalytic networks.

Allosteric regulation provides a particularly interesting candidate mechanism for such integration. Allostery describes the modulation of molecular activity or binding affinity through interactions that alter the conformational or energetic state of a macromolecule (Fenton 2008). Originally conceptualized as a fundamental principle of biological regulation (Monod 1977), allostery is now commonly interpreted through conformational ensemble models, in which ligand binding or other perturbations redistribute the relative populations of molecular states (Wodak et al. 2019). Importantly, allosteric regulation is not restricted to proteins. Experimental studies have demonstrated ligand-dependent conformational changes and catalytic modulation in engineered ribozymes (Araki 1998). These observations establish the physical plausibility of RNA-based allosteric mechanisms and suggest that conditional molecular regulation could have preceded the emergence of protein-based regulatory networks. In particular, ATP-dependent allostery could provide a mechanism linking the metabolic state of an RNA system to the activity and interactions of its replicating components.

In previous work, we developed mathematical models of early RNA-based autocatalytic systems to investigate the evolutionary dynamics of replication and molecular parasitism (Conrad et al. 2023; Pirovino et al. 2025). Using a Lotka–Volterra framework, we first demonstrated that tripartite systems comprising nested host–parasite interactions can exhibit homeostatic stability (Conrad et al. 2023). We subsequently extended this approach to autocatalytic ribozyme networks governed by Michaelis–Menten kinetics, showing that interactions among host, parasite, and hyperparasite catalysts can generate characteristic dynamical trajectories in which parasitic components become functionally integrated into the network (Pirovino et al. 2025). These findings suggest that molecular parasitism need not represent an exclusively destructive evolutionary force but may, under specific interaction architectures, contribute to the stabilization of autocatalytic systems.

Here, we extend this framework by coupling autocatalytic RNA replication to an ATP/ADP-based protometabolic energy cycle and ATP-dependent allosteric regulation. We investigate whether a minimal network comprising a replicating host ribozyme, a parasite-derived metabolic catalyst, and hyperparasite-mediated regulatory interactions can sustain replication despite the continual emergence of non-catalytic parasitic mutants. Our simulations identify a sequence of functional dependencies between energy conversion and molecular regulation. An initial increase in ATP/ADP turnover establishes conditions under which ATP-dependent allosteric regulation becomes effective. Hyperparasite-mediated regulation can then suppress parasite-driven network collapse, but ATP sequestration introduces an energetic constraint that requires further enhancement of ATP turnover for sustained replication. We additionally identify two alternative routes to effective parasite control: intrinsic allosteric responsiveness of parasitic ribozymes or conversion to an allosterically responsive state through an additional catalytic activity. Together, these findings demonstrate how energy conversion, information replication, and molecular regulation can become dynamically integrated within a minimal autocatalytic RNA network, providing a computational framework for investigating the emergence of stable, self-sustaining proto-Darwinian systems.

Results and Discussion

We construct a minimal model of an autocatalytic ribozyme network capable of maintaining stable self-replication during the transition from geochemical prebiotic chemistry toward an emerging proto-biological system. The minimal requirements are (i) a prebiotically available source of activated chemical energy, represented here by an ATP/ADP-based energy-conversion cycle (Pinna et al. 2022), and (ii) autocatalytic, template-based self-sustained replication (Papastavrou 2024; Gianni et al. 2026) that remains robust against the internal emergence of, or invasion by, parasitic ribozymes (Conrad et al. 2023; Pirovino 2025).

Here, we introduce a specific realization of the general framework described in the Methods section (Eqs. (1)–(7)), which we refer to as the minimal stable model**:** an autocatalytic RNA-world habitat regulated by an ATP/ADP-based energy cycle. The construction of this model relies on the following assumptions. Because ribozyme replication is driven by an ATP/ADP-based proto-metabolic energy cycle (Pinna et al. 2022), the habitat must maintain a sufficient ATP supply to sustain replication. However, any prebiotic habitat has limited access to both metabolic energy and the molecular resources required for RNA synthesis. Since ATP serves simultaneously as an energy carrier and as a molecular resource for replication, we assume conservation of the total ATP and ADP pools, including both free and ribozyme-bound forms. Accordingly, the conservation relation defined by Eq. (7) also applies to the minimal model, as schematically illustrated in Fig. 1. As a starting point, we consider the shortest possible autocatalytic ribozyme cycle, namely a type 2 cycle of length one:

$$R_1 + R_1 \underset{off''_{11}}{\overset{on''_{11}}{\rightleftharpoons}} Y''_{11} \underset{uch''_{11}}{\overset{ch''_{11}}{\rightleftharpoons}} Z''_{11} \xrightarrow{cat''(R_1)_{11}} R_1$$

Here, R_1 denotes the host replicase, which catalyzes its own replication. Throughout Fig. 2, we assume that replication of the host replicase is powered exclusively by an ATP/ADP-based chemical energy cycle naturally available within the habitat (Pinna et al. 2022). No ATP/ADP-cycle-catalyzing ribozyme is present at this stage. Consequently, free and total concentrations of ATP and ADP coincide, and the available ATP pool is directly coupled to replication of R_1 (Fig. 2a and b).

Despite its high standard free energy of hydrolysis of 50 kJ mol^{-1}, ATP is chemically stable, with an estimated half-life of approximately one year under aqueous physiological-like conditions. In extant organisms, the ratio [ATP]/[ADP][Pi] is maintained approximately nine orders of magnitude away from equilibrium, reflecting the active regulation of cellular energy metabolism (Macdonald 2025). Under prebiotic conditions, however, such a strong thermodynamic disequilibrium would initially have been much less pronounced. In our model, the phosphorylation potential is subsequently increased through the evolution of enhanced ATP/ADP-cycle turnover, as described in the following section.

Because replication of the host replicase is inevitably error-prone, catalytically inactive parasitic ribozymes R_3 continuously arise through mutation (Iranzo et al. 2016; Koonin 2017). In the absence of an effective regulatory mechanism, uncontrolled replication of these parasites by the host replicase ultimately leads to collapse of the host–parasite system (R_1, R_3), (Fig. 3a to c). A major source of this instability is the characteristic binding behavior of parasites. Throughout this work, we define the parasitic binding property as a combination of a relatively high association rate with the host replicase R_1, and very low association rates among parasitic ribozymes. As a result, parasitic ribozymes compete efficiently for access to the host replicase while exhibiting only weak self-association. This binding pattern gives rise to the characteristic evolutionary trajectory observed throughout our simulations: parasites initially proliferate at the expense of the host (Fig. 3c), but their continued expansion ultimately causes the collapse of both the host and parasite populations (Fig. 3b to c). Fig. 3 illustrate how the parasitic binding property, in the absence of any regulatory mechanism, inevitably drives the host–parasite system to collapse.

We propose allosteric regulation as a plausible evolutionary mechanism by which early autocatalytic RNA systems could have mitigated molecular parasitism. This hypothesis is supported by the widespread occurrence of allosteric regulation in extant biological systems (Montserrat-Canals et al. 2025). According to Eq. (6), each ribozyme R_{2k-1} may reversibly convert into an ATP-bound allosteric state, R_{2k}. The replicase R_1 is assumed to lack an allosteric site and is therefore not subject to allosteric regulation ($R_2 = 0$). This simplifying assumption isolates the effects of allosteric regulation on parasite control without introducing additional regulation of the replication process itself. Not all parasitic ribozymes are assumed to be allostery-prone. However, if a parasitic ribozyme R_3 undergoes ATP-induced conversion to the allosteric state R_4, thereby completing the allosteric conversion cycle defined by Eq. (6), uncontrolled parasite proliferation can be markedly attenuated (Fig. 4a to d), provided that R_4 possesses the assumed hyperparasitic binding property. In this scenario, allosteric regulation serves a dual evolutionary role. First, it suppresses runaway parasite proliferation. Second, rather than eliminating parasitic ribozymes, it creates an opportunity for their evolutionary exaptation into functional components of the molecular ecosystem, where they may ultimately contribute to host fitness.

The hyperparasitic binding property is characterized by three binding preferences: a high association rate with the host replicase R_1, comparable to that of the parasite R_3; a high association rate with ATP-free parasitic ribozymes R_3; and, optionally, an elevated association rate with ATP-bound parasitic ribozymes R_4. Consequently, ATP-bound parasites not only compete with ATP-free parasites for access to the host replicase but also bind directly to parasitic ribozymes, thereby suppressing their uncontrolled proliferation. This hyperparasitic strategy, however, incurs a metabolic cost. ATP sequestration by the allosteric state R_4reduces the concentration of free ATP, thereby slowing ATP–ADP turnover and progressively limiting the metabolic energy available to sustain RNA

replication. Consequently, the metabolic energy available to sustain RNA replication progressively becomes limiting. When the ATP–ADP turnover rate is increased by doubling the rate constants $k_0$and $k_1$in Eq. (3) relative to the conditions shown in Fig. 4a to d, complete stabilization is restored (Fig. 5a to d). This finding indicates that the residual destabilization results primarily from reduced ATP turnover caused by ATP sequestration, rather than from allosteric regulation per se. The simulations therefore demonstrate that allosteric regulation can provide an effective mechanism for suppressing molecular parasitism, provided that ATP–ADP turnover remains sufficiently rapid to sustain the energetic demands of RNA replication.

In the first scenario, loss of replicase activity is intrinsically coupled to the acquisition of an allosteric site. Consequently, every parasitic product of the host replicase R_1 immediately enters the allosteric conversion cycle described by Eq.(6). Fig. 4a to d and 5a to d demonstrate that this mechanism effectively stabilizes the host–parasite system. If such an intrinsic coupling were readily selectable in an RNA-world habitat, it would constitute the most energy-efficient solution to molecular parasitism.

The second scenario is energetically less efficient but is likewise supported by our simulations. In this scenario, a parasitic ribozyme, denoted R_5, evolves into an allosterase (Fig. 6d). For simplicity, we assume that the allosterase is itself allostery-prone and therefore possesses an ATP-bound allosteric counterpart, R_6 (Fig. 6e). Upon encounter, R_5, and possibly also R_6, catalyzes the conversion of a non-allostery-prone parasitic ribozyme R_3 into the allostery-prone forms R_7 and R_8 through a type 1 catalytic process (Fig. 6f to g). Figures 6a to g show that this mechanism substantially improves system stability relative to the unregulated dynamics shown in Fig. 3a to c. Complete stabilization, however, is not achieved because ATP sequestration during allosteric regulation slows ATP–ADP turnover, thereby limiting the metabolic energy available for RNA replication. When the ATP–ADP turnover rate is increased by tripling the rate constants k_0 and k_1, complete stabilization is restored (Fig. 7a to g).

Taken together, these simulations demonstrate that two distinct evolutionary pathways can stabilize RNA replication in the presence of molecular parasitism. The first relies on intrinsic allostery-proneness, in which all newly emerging parasitic ribozymes are inherently capable of ATP-dependent allosteric regulation (Fig. 4 and 5). The second relies on allosterase-mediated regulation, in which a specialized allosterase converts non-allostery-prone parasitic ribozymes into allostery-prone forms (Fig. 6 and 7). In both scenarios, molecular parasitism is tamed through ATP-dependent allosteric regulation. However, ATP sequestration by the allosteric states reduces the effective ATP–ADP turnover rate, thereby imposing an energetic cost on the system.

The simulations presented above show that allosteric regulation effectively tames molecular parasitism but simultaneously reduces the metabolic energy supply by sequestering ATP. This trade-off creates a selective pressure favoring ribozymes that restore ATP–ADP turnover. We therefore propose that, among the predominantly catalytically inactive parasitic ribozymes, one mutant R_3 acquires catalytic activity for the ATP–ADP cycle (type 3), thereby functioning as an ATP synthase/ATPase (Fig. 8a to d).

Following the first evolutionary scenario described in the previous section, we assume that this ATP synthase/ATPase ribozyme is itself allostery-prone and therefore possesses the ATP-bound allosteric counterpart R_4. As shown in Fig. 4 and 5, allosteric regulation alone substantially improves the stability of the host–parasite system but does not achieve complete stabilization because ATP sequestration slows ATP–ADP turnover. By simultaneously catalyzing ATP regeneration, R_3 compensates for this reduction in ATP turnover, thereby restoring the metabolic energy supply required for RNA replication and enabling complete stabilization of the system.

The allosteric regulation of the ATP synthase/ATPase ribozyme R_3 serves two complementary functions, namely first, control of molecular parasitism**.** The ATP-loaded allosteric counterpart R_4 attenuates the parasitic behavior of R_3 through the hyperparasitic binding property. Second, regulation of ATP availability. Because R_4 is catalytically inactive, ATP bound to its allosteric site is temporarily removed from the metabolically active pool. The allosteric counterpart therefore acts as a dynamic ATP buffer, regulating ATP availability while R_3 maintains ATP–ADP turnover. Together, these two functions establish a feedback mechanism in which ATP synthase/ATPase activity maintains the metabolic energy supply required for RNA replication, whereas allosteric regulation prevents uncontrolled proliferation of parasitic ribozymes.

The present study identifies a minimal autocatalytic RNA network in which information replication, ATP/ADP-based energy conversion, and molecular regulation become dynamically integrated. Our simulations demonstrate that sustained replication in the presence of continually emerging parasitic ribozymes can be achieved through the combined activity of a self-replicating host, an ATP/ADP-cycle-catalyzing ribozyme, and ATP-dependent allosteric regulation mediated by hyperparasitic interactions. Within the modeled reaction architecture, these components establish a self-maintaining system in which molecular parasitism is constrained without eliminating the parasitic intermediates that may contribute to metabolic and regulatory functions.

A central finding is the energetic trade-off associated with allosteric parasite control. Although ATP-dependent allostery suppresses the proliferation of non-catalytic parasites, ATP sequestration by allosteric ribozymes reduces the free ATP pool and constrains energy turnover. Consequently, effective regulation alone is insufficient to guarantee sustained replication. Stabilization requires adequate ATP regeneration, achieved in our model either through increased turnover of the pre-existing energy cycle or through the introduction of a parasite-derived ribozyme catalyzing ATP/ADP interconversion. The resulting feedback between energy conversion and parasite suppression illustrates how metabolic and regulatory functions can become mutually dependent rather than evolving as independent molecular capabilities.

These findings suggest an evolutionary role for molecular parasitism extending beyond its conventional interpretation as a destabilizing consequence of imperfect replication. Parasitic variants generate a selective challenge that may favor mechanisms capable of restricting their proliferation, while the energetic costs of such mechanisms create additional demands for metabolic adaptation. Our simulations are consistent with a sequence in which sufficient initial energy throughput enables regulatory control, and subsequent improvements in energy conversion compensate for the costs imposed by regulation. This relationship suggests a control-before-optimization principle: increasing catalytic or energetic efficiency in an unregulated system may amplify parasitic exploitation, whereas regulatory mechanisms can establish conditions under which further metabolic improvements benefit network persistence. This interpretation parallels broader theories of evolutionary transitions, in which the suppression of internal conflict facilitates the emergence of higher levels of biological organization (Maynard Smith 1995; Szathmáry 2015).

The model identifies two alternative architectures for ATP-dependent parasite control. In the first, loss of replicase activity is associated with intrinsic allosteric responsiveness, allowing parasitic ribozymes to participate directly in hyperparasitic regulation. In the second, a specialized allosterase catalyzes the conversion of non-allostery-prone parasites into allostery-prone forms. Both architectures support stable replication under appropriate energetic conditions, including following successive rounds of parasite emergence. Their principal distinction lies

in the additional catalytic machinery required by the allosterase-mediated pathway. These results indicate that the regulatory function necessary for network stabilization need not depend on a single molecular architecture, although the evolutionary accessibility of either mechanism remains to be established.

The present work extends our previous models of nested host–parasite interactions (Conrad et al. 2023; Pirovino et al. 2025) by explicitly coupling RNA replication and molecular parasitism to an ATP/ADP-based energy cycle and ligand-dependent allosteric regulation. Whereas earlier models demonstrated that hyperparasitic interactions can stabilize autocatalytic networks under externally supplied energetic conditions, the present framework introduces feedback between ATP availability, metabolic catalysis, and the regulatory interactions governing parasite proliferation. This extension provides a mechanistic basis for investigating how parasitic components may become functionally integrated into the metabolic and regulatory organization of early replicating systems.

Several limitations should be acknowledged. The model represents an idealized chemical network with predefined catalytic activities, binding preferences, and allosteric responses. It therefore establishes the dynamical feasibility of the proposed mechanisms rather than demonstrating their spontaneous molecular emergence or historical evolutionary sequence. The ATP/ADP cycle similarly represents an abstraction of protometabolic energy conversion, whose operation in a prebiotic environment would require an appropriate source of chemical free energy. Furthermore, the stability of the network depends on the modeled reaction architecture and kinetic parameters. Experimental characterization of RNA-based allosteric interactions, parasite-derived metabolic catalysis, and their energetic coupling would be required to evaluate the biochemical accessibility of the proposed mechanisms.

Our results suggest that the evolutionary significance of early molecular regulation may have extended beyond the suppression of parasites: by constraining molecular exploitation, regulation could have created the conditions under which improved energy conversion and replication became mutually reinforcing, enabling the emergence of persistent, evolvable RNA systems.

Materials and Methods

We consider an RNA-world habitat in which an underlying proto-metabolism provides sufficient chemical energy to sustain the production and maintenance of a limited set of ribozymes. These ribozymes are assumed to self-organize into autocatalytic networks.

In this section, we formulate the reaction equations of a general mathematical framework describing autocatalytic ribozyme networks fueled and regulated by an ATP/ADP-based energy cycle supplied by the surrounding habitat. The framework permits an arbitrary number of distinct ribozyme species participating in an autocatalytic replication network and provides the basis for the minimal model developed in the Results section.

Let n be the number of different ribozymes, $R_1, R_2, \ldots, R_n$, the free ribozyme concentrations, and $d_{R_i}, i = 1, \ldots, n$, the decay rates of these ribozymes.

These ribozymes may exhibit three fundamentally distinct catalytic functions, which we refer to here as the three types of catalysis.

Type 1 catalysis – RNA modification

A catalytically active ribozyme modifies a substrate ribozyme to produce a different ribozyme. During this process, the catalyst forms a transient intermediate complex with the substrate ribozyme, which is chemically transformed into the reaction product.

Type 2 catalysis – template-directed replication

A catalytically active ribozyme uses another ribozyme as a template for the synthesis of a new ribozyme. The catalyst therefore forms a transient intermediate complex with the template ribozyme. Upon completion of replication, both the catalyst and the template are released unchanged, while the newly synthesized ribozyme enters the habitat as an additional product.

Type 3 catalysis – metabolic energy conversion

A catalytically active ribozyme catalyzes the interconversion of non-genetic substrates, such as ATP, ADP, or other small molecules involved in proto-metabolism. In contrast to Types 1 and 2, neither the substrates nor the products are information-carrying RNA molecules. Instead, these reactions generate or recycle the chemical energy and molecular resources required to sustain autocatalytic ribozyme replication.

In the present work, modeling of type 1 catalytic processes is restricted to hypothetical allosterases involved in allosteric ATP regulation of ribozymes. Although type 1 processes, including ligase- and recombinase-mediated RNA modification, were likely important during the emergence of template-based replication (type 2 catalysis), the present model focuses on the minimal autocatalytic pathway required to sustain replication. Within this framework, stable self-replication is achieved through the coupled action of type 2 and type 3 catalytic processes, while type 1 catalysis is considered only as a regulatory mechanism for controlling parasitic ribozymes.

Definitions of type 1 and type 2 catalytic processes

We first define the concentrations and rate processes associated with type 1 and type 2 ribozyme activities. Throughout the model, we use the general reaction scheme

$$R + S \rightleftharpoons RS \rightleftharpoons RS^* \rightarrow RP \rightarrow R + P,$$

where RS denotes the reversibly bound ribozyme–substrate complex, RS^* the activated catalytic complex, and RP the ribozyme–product complex. The activated catalytic complex RS^* is explicitly represented in the model, whereas the ribozyme–product complex RP is not. Throughout this work, the term "charged" refers to the activated ribozyme–substrate state RS^*, whereas "uncharged" refers to the reversibly bound ribozyme–substrate complex RS.

Let $Y', Z', Y'', Z'' \epsilon\ \mathbb{R}^{nxn}$ be matrices. For $i, j = 1, .., n$ the entries of these matrices are defined as follows:

Y'_{ij} … uncharged type 1 intermediate complex of ribozyme R_i with substrate R_j, being subject to modification,

Z'_{ij} … charged type 1 intermediate complex of ribozyme R_i with substrate R_j, being subject to modification,

Y''_{ij} … uncharged type 2 intermediate complex of ribozyme R_i with template R_j,

Z''_{ij} … uncharged type 2 intermediate complex of ribozyme R_i with template R_j

We note that in general $Y'_{ij} \neq Y'_{ji}$, $Z'_{ij} \neq Z'_{ji}$, $Y''_{ij} \neq Y''_{ji}$, and $Z''_{ij} \neq Z''_{ji}$. This stems from the fact that for both type 1 and type 2 intermediate complexes the roles of R_i and R_j are distinct, and thus not exchangeable: R_i acts as the enzyme catalyzing the reproduction, and R_j functions as type 1 substrate subject to modification or as type 2 template.

In both cases, type 1 and 2, these concentrations are governed by a respective Michaelis-Menten process:

$$R_i + R_j \underset{off'_{ij}}{\overset{on'_{ij}}{\rightleftharpoons}} Y'_{ij} \underset{uch'_{ij}}{\overset{ch'_{ij}}{\rightleftharpoons}} Z'_{ij} \overset{cat'(R_k)_{ij}}{\rightharpoonup} R_k, \qquad i,j,k = 1,\dots,n, \quad (1)$$

$$R_i + R_j \underset{off''_{ij}}{\overset{on''_{ij}}{\rightleftharpoons}} Y''_{ij} \underset{uch''_{ij}}{\overset{ch''_{ij}}{\rightleftharpoons}} Z''_{ij} \overset{cat''(R_k)_{ij}}{\rightharpoonup} R_k, \qquad i,j,k = 1,\dots,n. \quad (2)$$

Here, the different classes of kinetic parameters—namely association (on) rates, dissociation (off) rates, charging (activation) rates, discharging/uncharging (deactivation) rates, and catalytic rates—are encoded as entries of $n \times n$ matrices. For instance, for $n = 2$, the type 1 association-rate matrix is defined as:

$$on' = \begin{pmatrix} on'_{11} & on'_{12} \\ on'_{21} & on'_{22} \end{pmatrix}.$$

We write the n x n matrix $on' = \left[on'_{ij}\right]_{ij} \in \mathbb{R}^{nxn}$, implying $i,j = 1,\dots,n$.

Thus, we define the following type 1 and 2 matrices of the rates:

$off' = \left[off'_{ij}\right]_{ij}, off'' = \left[off''_{ij}\right]_{ij} \in \mathbb{R}^{nxn}$… off-rates from uncharged type 1 and 2 intermediate complexes to free ribozymes,

$ch' = \left[ch'_{ij}\right]_{ij}, ch'' = \left[ch''_{ij}\right]_{ij} \in \mathbb{R}^{nxn}$… charge-rates from uncharged to the charged type 1 and 2 intermediate complexes,

$uch' = \left[uch'_{ij}\right]_{ij}, uch'' = \left[uch''_{ij}\right]_{ij} \in \mathbb{R}^{nxn}$… uncharge-rates from the charged to uncharged type 1 and 2 intermediate complexes.

We define the catalytic rates as follows. Let $cat'(R_1) = \left[cat'(R_1)_{ij}\right]_{ij} \in \mathbb{R}^{n\times n}$ denote the matrix of rates at which charged type 1 intermediate complexes catalyze the formation of ribozyme R_1. More generally, we define

$$cat'(R_k) = \left[cat'(R_k)_{ij}\right]_{ij} \in \mathbb{R}^{n\times n}, cat''(R_k) = \left[cat''(R_k)_{ij}\right]_{ij} \in \mathbb{R}^{n\times n},$$

as the matrices of rates at which charged type 1 and type 2 intermediate complexes, respectively, catalyze the formation of ribozyme $R_k, k = 1,\dots,n$.

Within this framework, each charged intermediate complex may catalyze the production of any free ribozyme species, either (i) through modification of an existing ribozyme in the case of type 1 catalysis, or (ii) through mutation or imperfect template-based replication in the case of type 2 catalysis.

Consequently, each free ribozyme species may receive contributions to its production from every charged intermediate complex. In practice, however, most entries *of* $cat'(R_k)$ and $cat''(R_k)$ are expected to be zero or negligibly small for all $k, i, j = 1, \dots, n$.

Finally, let $d_{Y'_{ij}}$, $d_{Z'_{ij}}$, $d_{Y''_{ij}}$, and $d_{Z''_{ij}}$, $i, j = 1, \dots, n$, denote the decay rates of the corresponding catalytic intermediate complexes.

The ATP-ADP cycle and its type 3 catalytic process

We now introduce two further concentrations, T and D, responsible for the energy supply in the habitat providing the metabolism needed for ribozyme reproduction.

T … concentration of free ATP in the habitat, and

D … concentration of free ADP in the habitat.

These concentrations are governed by the following reaction equation:

$$T \underset{k_1}{\overset{k_0}{\rightleftharpoons}} D \qquad (3)$$

We assume that the total amount of ADP and ATP in the habitat remains constant, including both free and bound forms. This constraint defines the external metabolic conditions for the reproduction cycle of the ribozymes R_i. The ATP–ADP cycle (3) is further assumed to be linked to the Michaelis–Menten processes (1) and (2) through two coupling pathways.

The first coupling between cycles (3), (1), and (2). We assume that the catalytic Michaelis–Menten processes (1) and (2) are driven by the ATP–ADP cycle (3) as follows. The activation of intermediate complexes formed between two ribozymes R_i and R_j, from the uncharged to the charged state, requires ATP consumption. For type 1 and type 2 processes, this activation is represented by:

$$Y'_{ij} \overset{ch'_{ij}}{\rightharpoonup} Z'_{ij}, \text{ and } Y''_{ij} \overset{ch''_{ij}}{\rightharpoonup} Z''_{ij}, \; i, j = 1, \dots, n,$$

During these transitions, ATP is hydrolyzed to ADP. Consequently, the production of an additional amount $\Delta Z'_{ij}$ or $\Delta Z''_{ij}$ requires the consumption of a corresponding amount of ATP, denoted by $\Delta T'$ and $\Delta T''$, respectively. These quantities are determined by the following equations:

$$\Delta T' = \alpha'_{ij} \Delta Z'_{ij}, \text{ and } \Delta T'' = \alpha''_{ij} \Delta Z''_{ij}, \; i, j = 1, \dots, n.$$

Here, the matrices $\alpha' = \left[\alpha'_{ij}\right]_{ij}$ and $\alpha'' = \left[\alpha''_{ij}\right]_{ij} \in \mathbb{R}^{n \times n}$ contain the coefficients specifying the ATP requirements of the charging processes described by reactions (1) and (2), respectively.

The second coupling between cycle (3) and processes (1) and (2). We assume that some, or potentially all, ribozymes R_i can contribute to the catalysis of the ATP–ADP cycle by enhancing both the synthesis of ATP and its hydrolysis into ADP. Following the definition introduced above, these reactions are classified as type 3 catalytic processes:

$Y'''(D)_i$ … concentration of uncharged type 3 ribozyme-ADP intermediate complex,

$Z'''(D)_i$ … concentration of charged type 3 ribozyme-ADP intermediate complex,

$Y'''(T)_i$ … concentration of uncharged type 3 ribozyme-ATP intermediate complex,

$Z'''(T)_i$ … concentration of charged type 3 ribozyme-ATP intermediate complex, $i = 1, \dots, n$.

The catalysis of this metabolic cycle is governed by Michaelis–Menten kinetics in both the forward and reverse directions. Considering first the direction of ATP production:

$$R_i + D \underset{off'''(D)_i}{\overset{on'''(D)_i}{\rightleftharpoons}} Y'''(D)_i \underset{uch'''(D)_i}{\overset{ch'''(D)_i}{\rightleftharpoons}} Z'''(D)_i \overset{cat'''(T)_i}{\rightharpoonup} T, \qquad i = 1, \dots, n, \qquad (4)$$

and second the direction of ATP-consumption and-hydrolysis, respectively:

$$R_i + T \underset{off'''(T)_i}{\overset{on'''(T)_i}{\rightleftharpoons}} Y'''(T)_i \underset{uch'''(T)_i}{\overset{ch'''(T)_i}{\rightleftharpoons}} Z'''(T)_i \overset{cat'''(D)_i}{\rightharpoonup} D, \qquad i = 1, \dots, n, \qquad (5)$$

Here, the vectors $on'''(D)$, $off'''(D)$, $ch'''(D)$, $uch'''(D)$, $cat'''(T)$, $on'''(T)$, $off'''(T)$, $ch'''(T)$, $uch'''(T)$, and $cat'''(D) \in \mathbb{R}^n$ represent the corresponding parameter entries for the additional type 3 Michaelis–Menten processes. As before, the transition of intermediate complexes from the uncharged to the charged state requires activation; in the case of ATP production, this process is given by:

$$Y'''(D)_i \overset{ch'''(D)_i}{\rightharpoonup} Z'''(D)_i, \qquad i = 1, \dots, n,$$

and in the case of ATP-hydrolysis

$$Y'''(T)_i \overset{ch'''(T)_i}{\rightharpoonup} Z'''(T)_i, \qquad i = 1, \dots, n,$$

additional amounts of ATP, i.e. $\Delta T's$, are needed for the catalyzation of the respective processes. ΔT in the case of ATP-production is

$$\Delta T = \alpha'''(D)_i \Delta Z'''(D)_i, \quad i = 1, \dots, n,$$

and in the case of ATP-hydrolysis

$$\Delta T = \alpha'''(T)_i \Delta''' Z(T)_i, \quad i = 1, \dots, n.$$

Again, $d_{Y'''(D)_i}$, $d_{Z'''(D)_i}$, $d_{Y'''(T)_i}$, and $d_{Z'''(T)_i}$, $i = 1, \dots, n$, represent the decay rates of the catalytic type 3 intermediate complexes formed between ribozymes and ADP or ATP, respectively.

The habitat restriction in the ATP-ADP cycle

The ATP demand rate T_{demand}, representing the amount of ATP that must be hydrolyzed to ADP per unit of time to maintain the complete charging process in the system, is therefore given by:

$$T_{demand} = \sum_{i,j=1}^{n} \{\alpha'_{ij} ch'_{ij} Y'_{ij} + \alpha''_{ij} ch''_{ij} Y''_{ij}\} + \sum_{i=1}^{n} \{\alpha'''(D)_i ch'''(D)_i Y'''(D)_i + \alpha'''(T)_i ch'''(T)_i Y'''(T)_i\}.$$

Conversely, the ATP–ADP cycle described by Eqs. (3), (4), and (5) determines the maximum total rate of ATP hydrolysis into ADP, which is given by:

$$T_{supply} = k_0 T + \sum_{i=1}^{n} cat'''(D)_i Z'''(T)_i .$$

If $T_{\mathrm{demand}} > T_{\mathrm{supply}}$, the resulting excess demand must be compensated for to restore equilibrium between ATP supply and consumption. To achieve this, all charging rates, ch'_{ij}, ch''_{ij}, $ch'''(D)_i$, and $ch'''(T)_i$, are proportionally reduced by multiplication with a common damping factor δ:

$$\delta = \min\left(\frac{T_{supply}}{T_{demand}}, 1\right) =$$

$$\min\left(\frac{k_0 T + \sum_{i=1}^{n} cat'''(D)_i Z'''(T)_i}{\sum_{i,j=1}^{n}\{\alpha'_{ij} ch'_{ij} Y'_{ij} + \alpha''_{ij} ch''_{ij} Y''_{ij}\} + \sum_{i=1}^{n}\{\alpha'''(D)_i ch'''(D)_i Y'''(D)_i + \alpha'''(T)_i ch'''(T)_i Y'''(T)_i\}}, 1\right).$$

Allosteric ATP-regulation of ribozymes

In the following, we set $n = 2\,m$, corresponding to an even number of ribozymes in the system. To incorporate allosteric ATP regulation into the model of ribozyme production, we assume that ATP molecules can bind to a non-active allosteric site on the ribozyme.

$$R_{2k-1} + T \underset{b_k}{\overset{a_k}{\rightleftharpoons}} R_{2k} \qquad (6)$$

Here, a_k denotes the rate of allosteric ATP binding, and b_k the corresponding reverse rate, for $k = 1, \ldots, m$. This distinction gives rise to two classes of ribozymes: ATP-loaded species—hereafter referred to as "loaded" (activated)—and ATP-unloaded species—hereafter referred to as "unloaded" (deactivated)—with respect to their allosteric sites. Accordingly, we assume that ribozymes R_i with even indices $i = 2k$ are allosterically ATP-loaded, whereas ribozymes with odd indices $i = 2k - 1$ remain unloaded. We further note that ribozymes R_{2k-1} can interact with ATP in two distinct ways. Binding of ATP at the catalytic site results in the formation of a type 3 intermediate complex $Y'''_{2k-1}(T)$, whereas binding at the allosteric site converts the ribozyme into its corresponding loaded form R_{2k}.

An important property of the allosteric process described by Eq. (6) is that it is assumed to be non-catalytic. The transition between allosteric states is therefore not mediated by any of the three catalytic processes included in the model (types 1–3). In particular, type 1 catalysis does not modify the allosteric state of a ribozyme: ATP-loaded ribozymes cannot arise from ATP-free ribozymes, nor can ATP-free ribozymes be regenerated from ATP-loaded ribozymes, through type 1 catalytic reactions. Hence, type 1 catalysis does not contribute to the interconversion between ATP-loaded and ATP-free ribozyme populations. Based on this assumption, we define:

$$\frac{dT}{dt} = -k_0 T + k_1 D - T_{allo-bound} + T_{allo-released}$$

+ net release from intermediate complexes T with ribozymes R_i

+ catalytic production of T from intermediate complexes with ribozymes R_i with D,

and

$$\frac{dD}{dt} = k_0 T - k_1 D$$

+ net release from intermediate complexes D with ribozymes R_i

+ catalytic production of D from intermediate complexes with ribozymes R_i with T,

where

$$T_{allo-bound} = \sum_{k=1}^{m}\left\{a_k R_{2k-1}T + \sum_{i,j=1}^{n} cat''(R_{2k})_{ij}Z''_{ij}\right\},$$

$$T_{allo-released} =$$

$$\sum_{k=1}^{m}\Bigg\{b_k R_{2k} + d_{R_{2k}}R_{2k} + d_{Y'''(D)_{2k}}Y'''(D)_{2k} + d_{Z'''(D)_{2k}}Z'''(D)_{2k} + d_{Y'''(T)_{2k}}Y'''(T)_{2k} + d_{Y'''(T)_{2k}}Y'''(T)_{2k}$$

$$+ d_{Z'''(T)_{2k}}Z'''(T)_{2k} + \sum_{i=1}^{n}\left(d_{Y'_{i,2k}}Y'_{i,2k} + d_{Y'_{2k,i}}Y'_{2k,i} + d_{Z'_{i,2k}}Z'_{i,2k} + d_{Z'_{2k,i}}Z'_{2k,i}\right)$$

$$+ \sum_{i=1}^{n}\left(d_{Y''_{i,2k}}Y''_{i,2k} + d_{Y''_{2k,i}}Y''_{2k,i} + d_{Z''_{i,2k}}Z''_{i,2k} + d_{Z''_{2k,i}}Z''_{2k,i}\right)\Bigg\}.$$

In the last equation, we assume that ATP bound at the allosteric site is released into the habitat during the decay of the ATP-loaded ribozyme R_{2k}, regardless of whether the ribozyme is present as a free species or as part of an intermediate complex.

Let finally $F_i, i = 1, \dots n$, define the net conversion flow between the $R_{2k-1}{}'s$ and $R_{2k}{}'s$ according to Eq. (6):

$$F_{2k-1} = -a_k R_{2k-1}T + b_k R_{2k},$$

$$F_{2k} = -F_{2k-1}, \qquad k = 1, \dots, m.$$

Now we can define the chemical dynamics of the whole system completely.

The explicit governing Michaelis-Menten equations

All these considerations lead to the following explicit ordinary Michaelis-Menten differential equations.

First, for the ATP-ADP cycle:

$$\frac{dT}{dt} = -k_0 T + k_1 D - T_{allo-bound} + T_{allo-released} +$$

$$+\sum_{j=1}^{n} off'''(T)_j Y'''(T)_j - on'''(T)_j R_j T + d_{Y'''(T)_j}Y'''(T)_j + d_{Z'''(T)_j}Z'''(T)_j + cat'''(T)_j Z'''(D)_j,$$

$$\frac{dD}{dt} = k_0 T - k_1 D +$$

$$\sum_{j=1}^{n} off'''(D)_j Y'''(D)_j - on'''(D)_j R_j D + d_{Y'''(D)_j}Y'''(D)_j + d_{Z'''(D)_j}Z'''(D)_j + cat'''(D)_j Z'''(T)_j,$$

assuming that all ADP and ATP molecules bound to the catalytic intermediates are released into the habitat during the decay of their intermediate complexes, and

$$\frac{d}{dt}Y'''(D)_i = -d_{Y'''(D)_i}Y'''(D)_i + on'''(D)_i R_i D - (off'''(D)_i + \delta ch'''(D)_i)Y'''(D)_i + uch'''(D)_i Z'''(D)_i,$$

$$\frac{d}{dt}Z'''(D)_i = -d_{Z'''(D)_i}Z'''(D)_i + \delta ch'''(D)_i Y'''(D)_i - uch'''(D)_i Z'''(D)_i - cat'''(T)_i Z(D)_i,$$

$$\frac{d}{dt}Y'''(T)_i = -d_{Y'''(T)_i}Y'''(T)_i + on'''(T)_i R_i T - (off'''(T)_i + \delta ch'''(T)_i)Y'''(T)_i + uch'''(T)_i Z'''(T)_i,$$

$$\frac{d}{dt}Z'''(T)_i = -d_{Z'''(T)_i}Z'''(T)_i + \delta ch'''(T)_i Y'''(T)_i - uch'''(T)_i Z'''(T)_i - cat'''(D)_i Z'''(T)_i,$$

for $i = 1, \dots, n$.

Second, for the ribozymes:

$$\frac{d}{dt}R_i = -d_{R_i}R_i + F_i +$$
$$+off'''(D)_i Y'''(D)_i - on'''(D)_i R_i D + cat'''(T)_i Z'''(D)_i$$
$$+off'''(T)_i Y'''(T)_i - on'''(T)_i R_i T + cat'''(D)_i Z'''(T)_i$$
$$+\left\{\sum_{j=1}^{n} off'_{ij}Y'_{ij} - on'_{ij}R_iR_j + off'_{ji}Y'_{ji} - on'_{ji}R_jR_i + \sum_{j=1}^{n} off''_{ij}Y_{ij} - on''_{ij}R_iR_j + off''_{ji}Y''_{ji} - on''_{ji}R_jR_i\right.$$
$$\left.+\sum_{l,j=1}^{n} cat''(R_i)_{lj}Z''_{lj} + cat''(R_l)_{ij}Z''_{ij} + cat''(R_l)_{ji}Z''_{ji} + cat'(R_i)_{lj}Z'_{lj} + cat'(R_l)_{ij}Z'_{ij}\right\},$$

for $i = 1, \dots, n$;

and for the type 1 and 2 intermediate complexes, we have

$$\frac{d}{dt}Y'_{ij} = -d_{Y'_{ij}}Y'_{ij} + on'_{ij}R_iR_j - \left(off'_{ij} + \delta ch'_{ij}\right)Y'_{ij} + uch'_{ij}Z'_{ij},$$
$$\frac{d}{dt}Z'_{ij} = -d_{Z'_{ij}}Z'_{ij} + \delta ch'_{ij}Y'_{ij} - uch'_{ij}Z'_{ij} - \sum_{l=1}^{n} cat'(R_l)_{ij}Z'_{ij,}$$
$$\frac{d}{dt}Y''_{ij} = -d_{Y''_{ij}}Y''_{ij} + on''_{ij}R_iR_j - \left(off''_{ij} + \delta ch''_{ij}\right)Y''_{ij} + uch''_{ij}Z'_{ij},$$
$$\frac{d}{dt}Z''_{ij} = -d_{Z''_{ij}}Z''_{ij} + \delta ch''_{ij}Y''_{ij} - uch''_{ij}Z'_{ij} - \sum_{l=1}^{n} cat''^{(R_l)}{}_{ij}Z''_{ij},\ i,j = 1, \dots, n.$$

Finally, the total concentrations of the ribozymes, free plus bound, are given by

$$R_i^{tot} = R_i + Y'''(D)_i + Z'''(D)_i + Y'''(T)_i + Z'''(T)_i$$
$$+\sum_{j=1}^{n} Y'_{ij} + Y'_{ji} + Z'_{ij} + Z'_{ji} + Y''_{ij} + Y''_{ji} + Z''_{ij} + Z''_{ji}, i = 1, \dots, n,$$

and, consequently, for the total amounts of ADP and ATP, free plus bound, it follows:

$$D^{tot} = D + \sum_{i=1}^{n} Y'''(D)_i + Z'''(D)_i,$$
$$T^{tot} = T + \sum_{k=1}^{m} R_{2k}^{tot} + \sum_{i=1}^{n} Y'''(T)_i + Z'''(T)_i.$$

In the preceding analysis, we assumed that the external metabolism of the habitat constrains the total amount of these quantities to remain constant, such that:

$$\frac{d}{dt}(D^{tot} + T^{tot}) = 0. \qquad (7)$$

Supplementary Information

The online version contains supplementary material available at ( ).

Acknowledgements

We warmly thank Udo Seifert for helpful discussions and his insights into statistical thermodynamics.

Funding

No funding reported.

Data and Code Availability

The R code implementing the equations and reproducing the analyses presented in this study is available on https://github.com/BICC-UNIL-EPFL/energy-metabolism-and-hyperparasitism and is archived at https://doi.org/10.5281/zenodo.20408570.

Declarations

Conflict of interest

The authors declare no conflicts of interest.

References

Anet FAL (2004) The place of metabolism in the origin of life. Curr Opin Chem Biol 8:654–659. https://doi.org/10.1016/j.cbpa.2004.10.005

Araki M, Okuno Y, Hara Y, Sugiura Y (1998) Allosteric regulation of a ribozyme activity through ligand-induced conformational change. Nucleic Acids Res 26:3379–3384. https://doi.org/10.1093/nar/26.14.3379

Briones C, Stich M, Manrubia SC (2009) The dawn of the RNA world: toward functional complexity through liga tion of random RNA oligomers. RNA 15:743–749. https://doi.org/10.1261/rna.1488609

Buss LW (1987) The evolution of individuality. Princeton University Press, Princeton, NJ

Conrad B, Iseli C, Pirovino M (2023) Energy-harnessing problem solving of primordial life. PLoS One 18:e0281661. https://doi.org/10.1371/journal.pone.0281661

de Duve C (2005) ATP. In: Singularities: landmarks on the pathways of life. Cambridge University Press, Cam bridge, pp 25–40. https://doi.org/10.1017/CBO9780511614736.007

Eigen M (1971) Selforganization of matter and the evolution of biological macromolecules. Naturwissenschaften 58:465–523

Fenton AW (2008) Allostery: an illustrated definition for the 'second secret of life'. Trends Biochem Sci 33:420–425. https://doi.org/10.1016/j.tibs.2008.05.009

Gianni E, Kwok SLY, Wan CJK, et al (2026) A small polymerase ribozyme that can synthesize itself and its comple mentary strand. Science 391:1022–1028. https://doi.org/10.1126/science.adt2760

Gilbert W (1986) Origin of life: the RNA world. Nature 319:618. https://doi.org/10.1038/319618a0

Hardie DG, Scott JW, Pan DA, Hudson ER (2003) Management of cellular energy by the AMP-activated protein kinase system. FEBS Lett 546:113–120. https://doi.org/10.1016/S0014-5793(03)00560-X

Hayden EJ, Lehman N (2006) Self-assembly of a group I intron from inactive oligonucleotide fragments. Chem Biol 13:909–918. https://doi.org/10.1016/j.chembiol.2006.06.014

Iranzo J, Puigbò P, Lobkovsky AE, Wolf YI, Koonin EV (2016) Inevitability of genetic parasites. Genome Biol Evol 8:2856–2869. https://doi.org/10.1093/gbe/evw193

Kauffman SA (1986) Autocatalytic sets of proteins. J Theor Biol 119:1–24. https://doi.org/10.1016/S0022-5193(86)80047-9

Kirschning A (2022) On the evolutionary history of the twenty encoded amino acids. Chemistry 28:e202201419. https://doi.org/10.1002/chem.202201419

Koonin EV, Wolf YI, Katsnelson MI (2017) Inevitability of the emergence and persistence of genetic parasites caused by evolutionary instability of parasite-free states. Biol Direct 12:31. https://doi.org/10.1186/s13062-017-0202-5

Krakauer DC, Bertschinger N, Olbrich E, Ay N, Flack JC (2020) The information theory of individuality. Theory Biosci 139:209–223. https://doi.org/10.1007/s12064-020-00313-7

Macdonald JE, Ashby PD (2025) The molecular mechanism of ATP synthase constrains the evolutionary land scape of chemiosmosis. Biophys J 124:2103–2119. https://doi.org/10.1016/j.bpj.2025.05.017

Maynard Smith J, Szathmáry E (1995) The major transitions in evolution. W.H. Freeman (Spektrum), Oxford

Monod J (1977) Chance and necessity: essay on the natural philosophy of modern biology. Penguin Books, Lon don

Montserrat-Canals M, Cordara G, Krengel U (2025) Allostery. Q Rev Biophys 58:e5. https://doi.org/10.1017/S0033583524000209

Morowitz HJ (1999) A theory of biochemical organization, metabolic pathways, and evolution. Complexity 4:39–53. https://doi.org/10.1002/(SICI)1099-0526(199907/08)4:6<39::AID-CPLX8>3.0.CO;2-2

Nghe P (2025) A stepwise emergence of evolution in the RNA world. FEBS Lett 599:2706–2717. https://doi.org/10.1002/1873-3468.70065

Nowak MA (2006) Five rules for the evolution of cooperation. Science 314:1560–1563. https://doi.org/10.1126/science.1133755

Papastavrou N, Horning DP, Joyce GF (2024) RNA-catalyzed evolution of catalytic RNA. Proc Natl Acad Sci U S A 121:e2321592121. https://doi.org/10.1073/pnas.2321592121

Pinna S, Kunz C, Halpern A, et al (2022) A prebiotic basis for ATP as the universal energy currency. PLoS Biol 20:e3001437. https://doi.org/10.1371/journal.pbio.3001437

Pirovino M, Iseli C, Curran JA, Conrad B (2025) Biomathematical enzyme kinetics model of prebiotic autocatalytic RNA networks. PLoS Comput Biol 21:e1012162. https://doi.org/10.1371/journal.pcbi.1012162

Pross A (2004) Causation and the origin of life: metabolism or replication first? Orig Life Evol Biosph 34:307–321. https://doi.org/10.1023/B:ORIG.0000016446.51012.bc

Shah V, de Bouter J, Pauli Q, Tupper AS, Higgs PG (2019) Survival of RNA replicators is much easier in protocells than in surface-based, spatial systems. Life 9:65. https://doi.org/10.3390/life9030065

Szathmáry E (2015) Toward major evolutionary transitions theory 2.0. Proc Natl Acad Sci U S A 112:10104–10111. https://doi.org/10.1073/pnas.1421398112

Whicher A, Camprubi E, Pinna S, Herschy B, Lane N (2018) Acetyl phosphate as a primordial energy currency at the origin of life. *Orig Life Evol Biosph* 48:159–179. https://doi.org/10.1007/s11084-018-9555-8

Wiener N (1948) Cybernetics: or control and communication in the animal and the machine. MIT Press, Cam bridge, MA

Wimmer JLE, Vieira AdN, Xavier JC, Kleinermanns K, Martin WF, Preiner M (2021) The autotrophic core: an an

cient network of 404 reactions converts H_2, CO_2, and NH_3 into amino acids, bases, and cofactors. *Micro organisms* 9:458. https://doi.org/10.3390/microorganisms9020458

Wodak SJ, Paci E, Dokholyan NV, et al (2019) Allostery in its many disguises: from theory to applications. Struc ture 27:566–578. https://doi.org/10.1016/j.str.2019.01.003

Zimmermann J, Werner E, Sodei S, Moran J (2024) Pinpointing conditions for a metabolic origin of life: underly ing mechanisms and the role of coenzymes. Acc Chem Res 57:3032–3043. https://doi.org/10.1021/acs.accounts.4c00423

Figures

Fig. 1. Minimal ATP–ADP cycle (schematic evolution)

Fig. 1

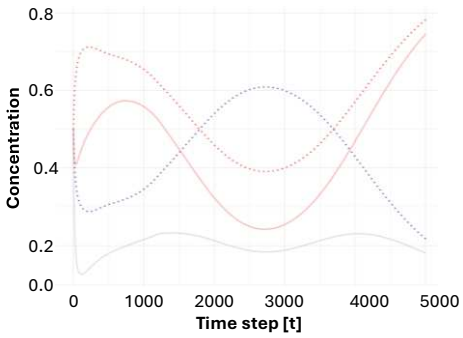


Fig. 2. Prebiotic ATP production and R_1 replication

Fig. 2

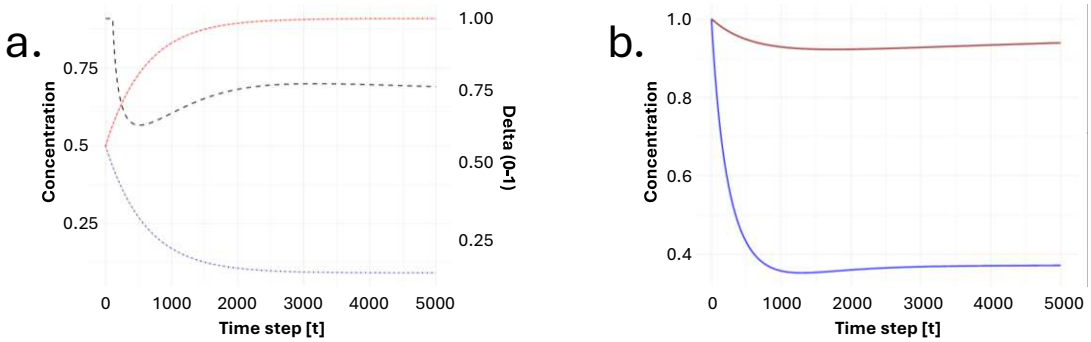


Fig. 3. Catalytically inactive parasitic ribozyme R_3

Fig. 3

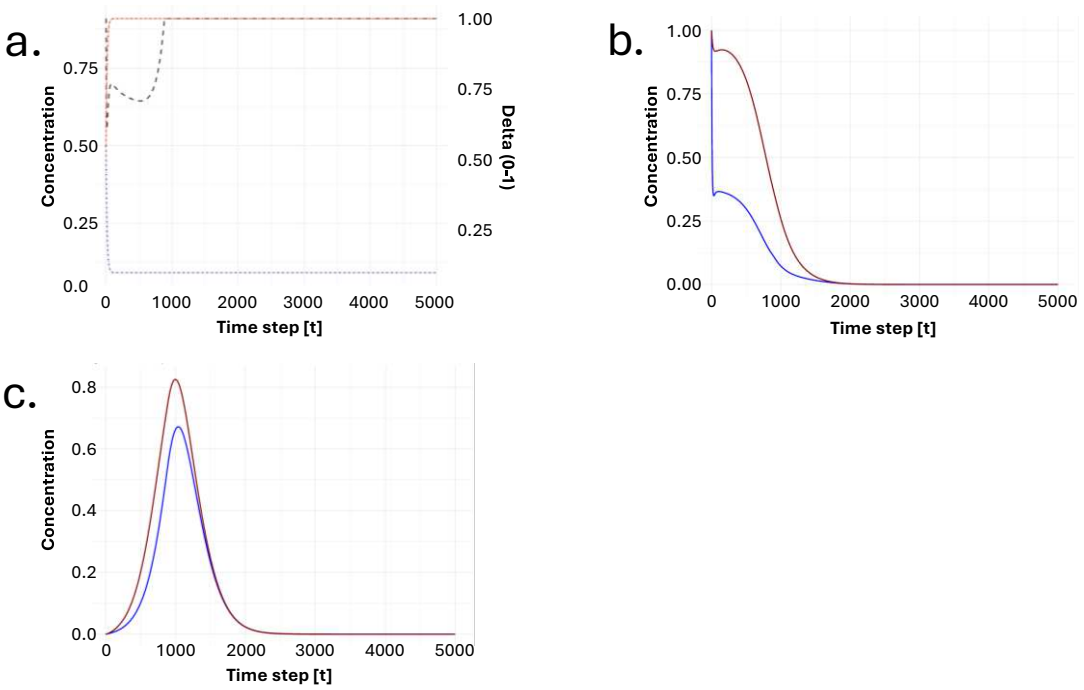


Fig. 4. Allosteric regulation mitigates molecular parasitism

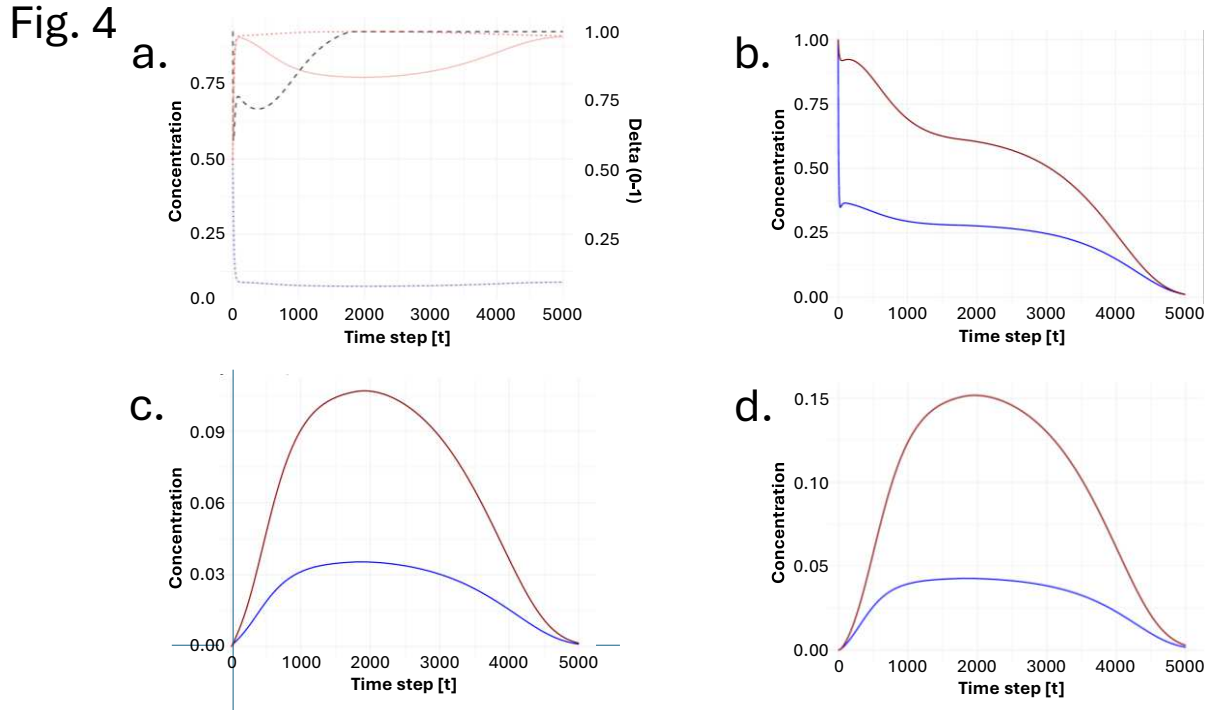


Fig. 5. Accelerating the ATP/ADP cycle restores stabilization

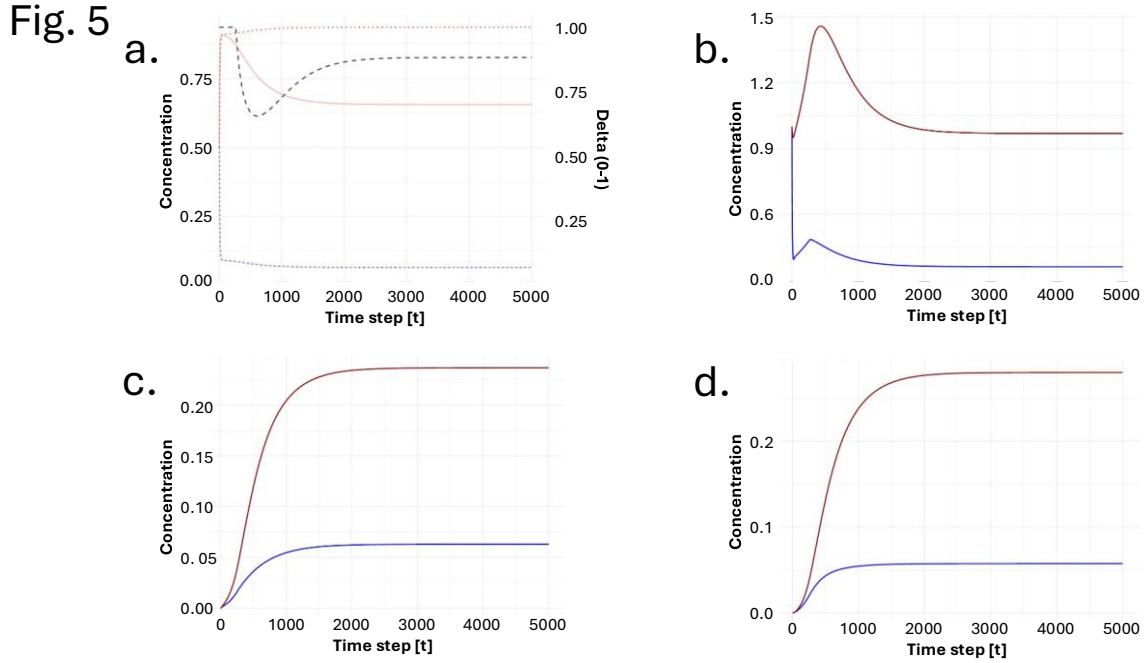


Fig. 6. Allosterases confer allostery in trans

Fig. 6

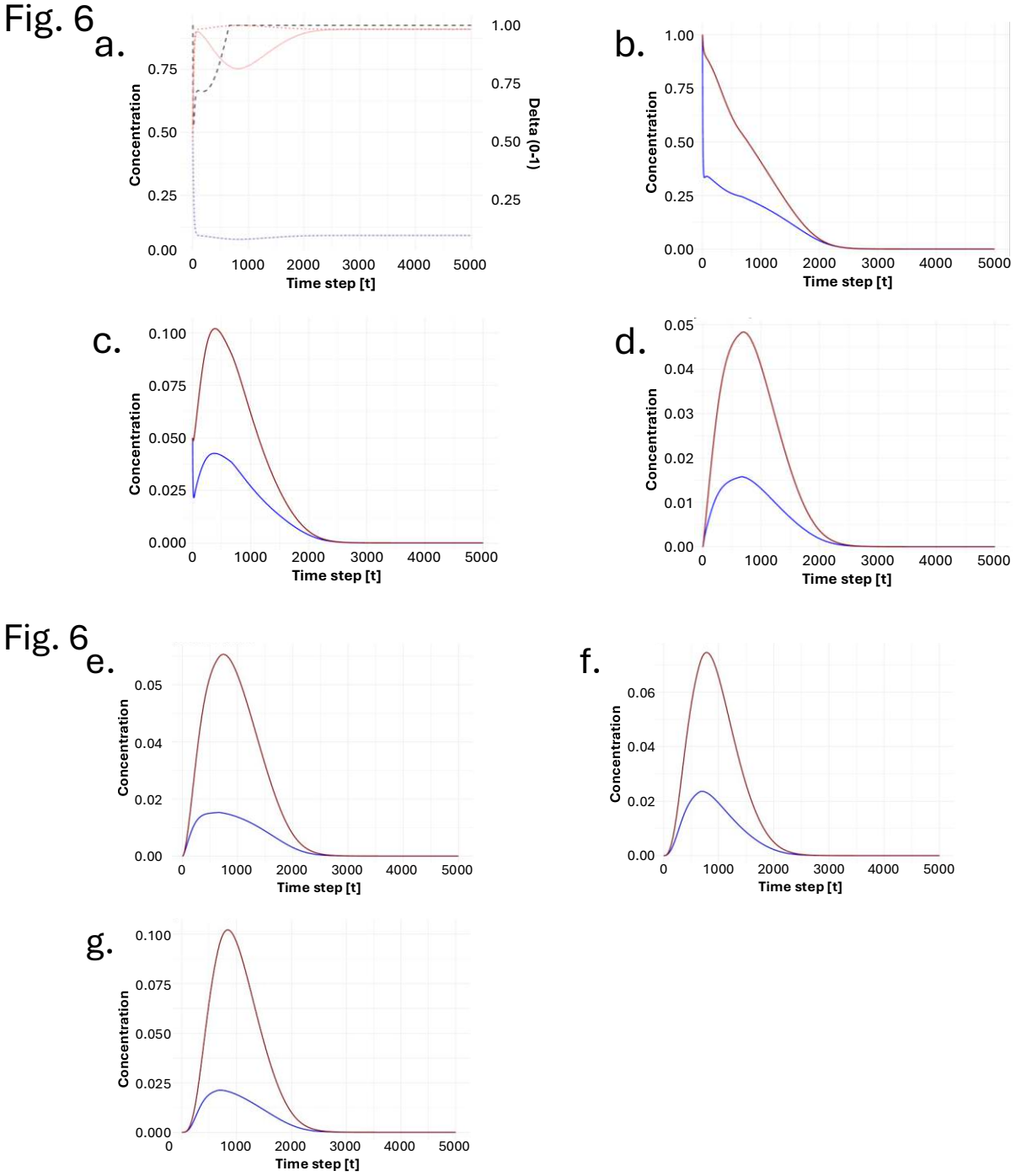


Fig. 7. Allosterases and enhanced ATP–ADP turnover

Fig. 7

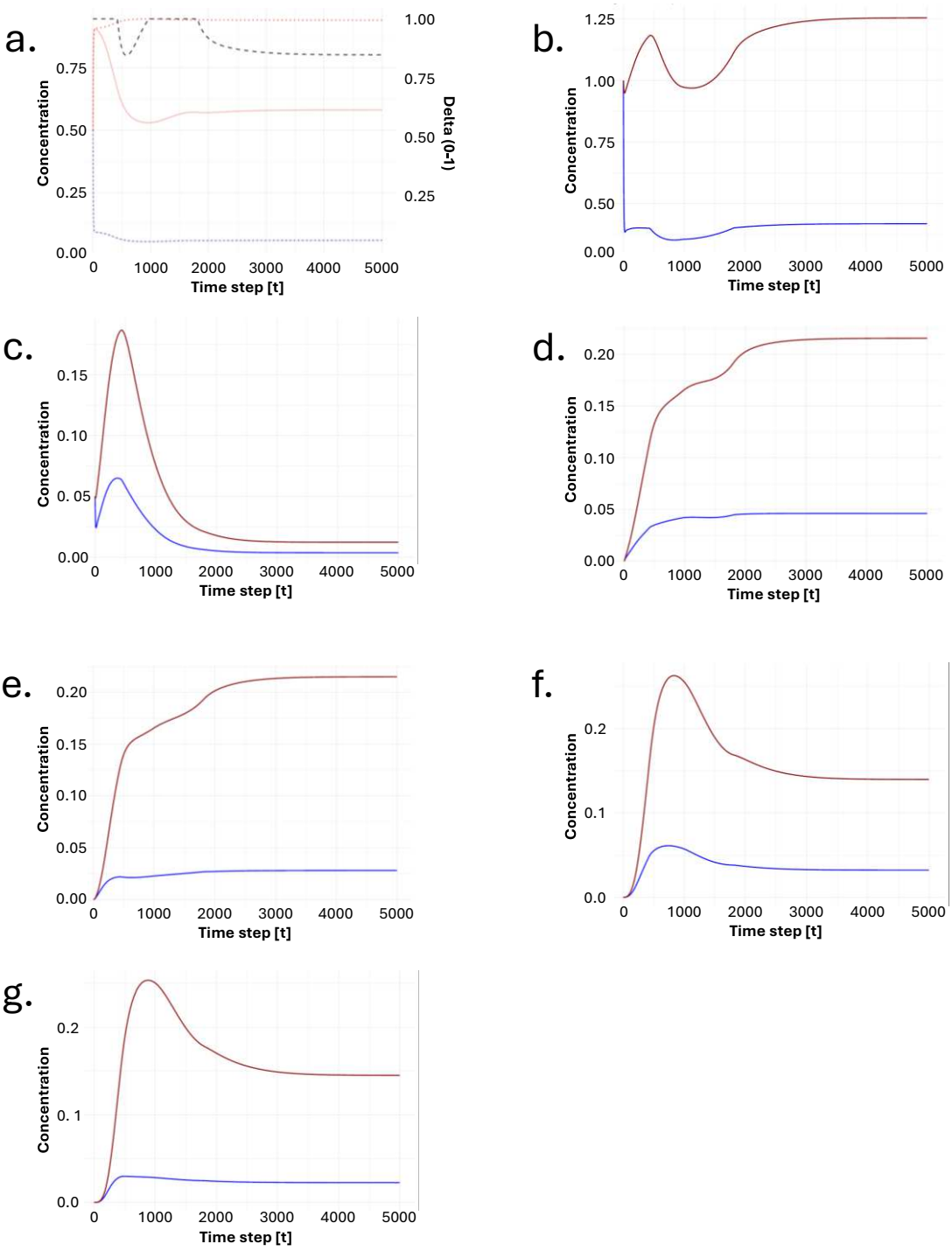


Fig 7

Fig. 8. Parasite ribozymes R_3 evolve into ATPase/ATP synthetase ribozymes

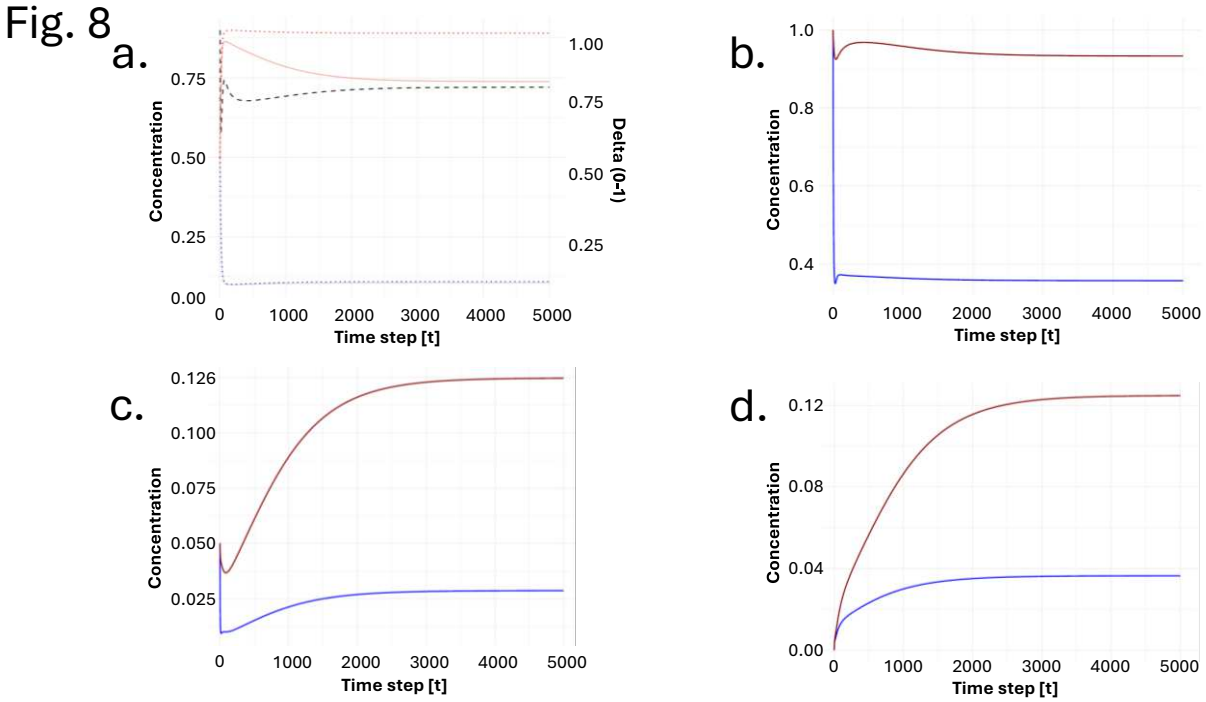


Fig. 9. ATPase/ATP synthase ribozymes enable resistance to subsequent parasite invasion

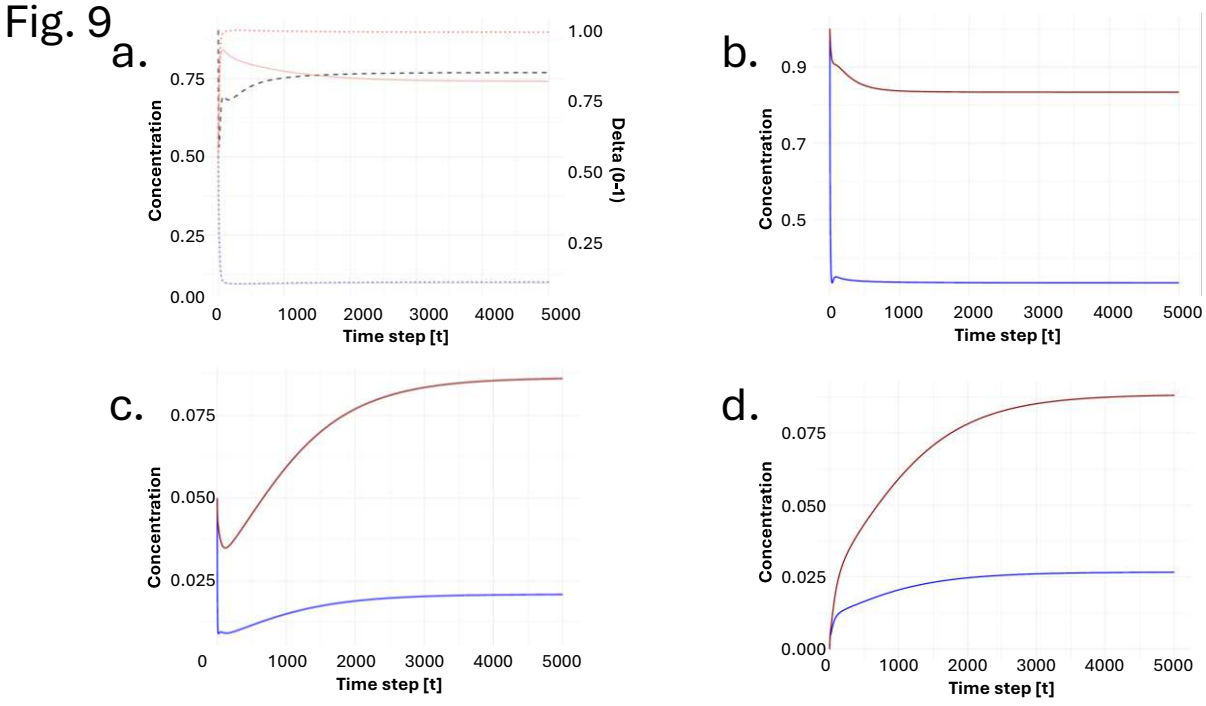


Fig. 9

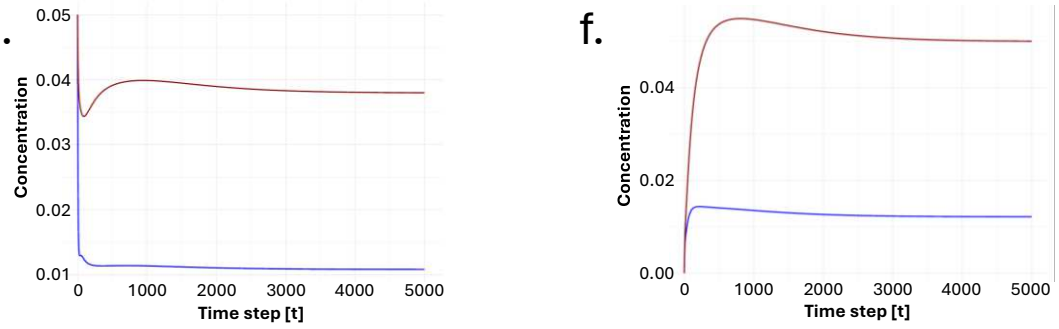


Fig. 10. Habitat with ATPase/ATP synthetase ribozymes and allosterases recapitulates parasite resistance

Fig. 10

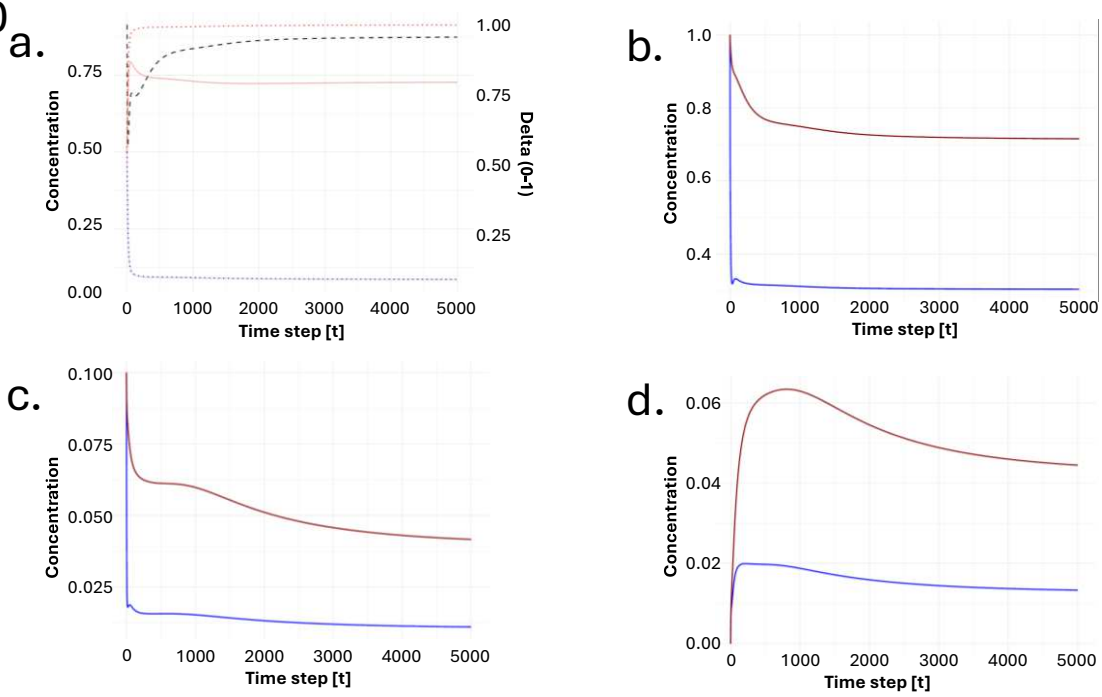


Fig. 10

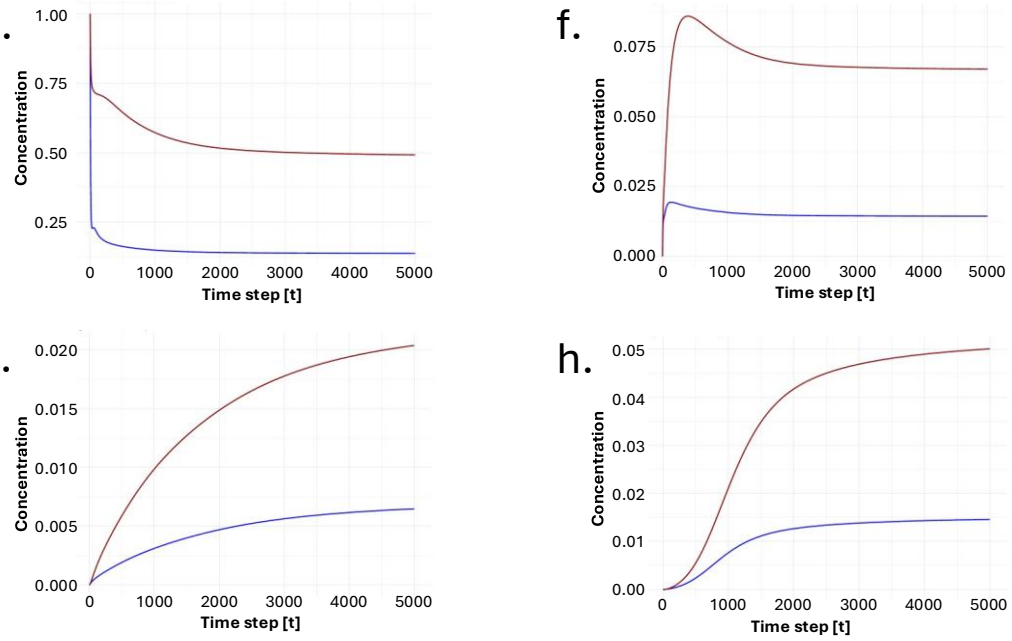


Figure Captions

Fig. 1. The habitat maintains a constant total nucleotide pool: $T_{\mathrm{tot}} + D_{\mathrm{tot}} = const$, with $T_{\mathrm{tot}} = T + (T_{tot} - T)$ and $D_{\mathrm{tot}} = D + (D_{tot} - D)$, with T, D denoting free and $(T_{\mathrm{tot}} - T), (D_{\mathrm{tot}} - D)$ bound ATP and ADP, respectively. The y-axis shows the concentrations of ATP and ADP ribozymes, and the x-axis represents discrete time steps.

Fig. 2. At moderate ATP consumption associated with replication, the system can be maintained without catalytic enhancement of the ATP–ADP cycle. **a** Free and total ATP and ADP concentrations are assumed to be identical. **b** All available ATP is immediately consumed by R_1replication. (D_—), (D_tot – –), (delta_—), (T_—), (T_tot– –); (R_1, blue; total $R_{1,\mathrm{tot}}$, brown).

Fig. 3. a Evolution of ADP (D_), ATP (T_), and (delta_); no ATP/ADP-cycle-catalyzing ribozyme is present at this stage. Initially, R_3 proliferates at the expense of the host **c**. However, unchecked parasite growth eventually causes the collapse of both the host R_1population **b**, and the R_3parasite population **c**. (D_—), (D_tot – –), (delta_—), (T_—), (T_tot– –); (R_1, blue; total $R_{1,\mathrm{tot}}$, brown; R_3, blue; total $R_{3,\mathrm{tot}}$, brown).

Fig. 4. Allosteric regulation mitigates molecular parasitism

a Evolution of ADP (D_), ATP (T_), and (delta_); no ATP/ADP-cycle-catalyzing ribozyme is present at this stage. **b** Evolution of the host ribozyme R_1. **c-d** The parasitic ribozyme R_3undergoes ATP-induced allosteric conversion to R_4, thereby substantially taming uncontrolled parasite proliferation, provided that R_4satisfies the hyperparasitic binding property. (D_—), (D_tot – –), (delta_—), (T_—), (T_tot– –); (R_1, blue; total $R_{1,\mathrm{tot}}$, brown; R_3, blue; total $R_{3,\mathrm{tot}}$, brown, R_4, blue; total $R_{4,\mathrm{tot}}$, brown).

Fig. 5. Accelerating the ATP/ADP cycle restores stabilization

a Evolution of ADP (D_), ATP (T_), and (delta_); no ATP/ADP-cycle-catalyzing ribozyme is present at this stage, but the ATP–ADP turnover rate is doubled. This increase, achieved by doubling the rate constants $k_0$and k_1, restores complete stabilization. **b-d** Evolution of the host ribozyme R_1, parasitic ribozyme R_3, and allosteric ribozyme R_4, respectively. (D_—), (D_tot – –), (delta_—), (T_—), (T_tot– –); (R_1, blue; total $R_{1,\mathrm{tot}}$, brown; R_3, blue; total $R_{3,\mathrm{tot}}$, brown, R_4, blue; total $R_{4,\mathrm{tot}}$, brown).

Fig. 6. Allosterases confer allostery in trans

a Evolution of ADP (D_), ATP (T_), and (delta_), no ATP/ADP-cycle-catalyzing ribozyme is present at this stage. The allosterase R_5 undergoes ATP-induced conversion to its allosteric counterpart R_6, which subsequently converts parasitic ribozymes R_3 into the allostery-prone forms R_7 and R_8. This mechanism improves system stability but does not achieve complete stabilization. **b-g** Evolution of R_1, R_3, R_5, R_6, R_7, and R_8, respectively. (D_—), (D_tot – –), (delta_—), (T_—), (T_tot– –); (R_1, blue; total $R_{1,\mathrm{tot}}$, brown; R_3, blue; total $R_{3,\mathrm{tot}}$, brown; R_5, blue; total $R_{5,\mathrm{tot}}$, brown; R_6, blue; total $R_{6,\mathrm{tot}}$, brown; R_7, blue; total $R_{7,\mathrm{tot}}$, brown; R_8, blue; total $R_{8,\mathrm{tot}}$, brown).

Fig. 7. Allosterases and enhanced ATP–ADP turnover

a Evolution of ADP (D_), ATP (T_), and (delta_), no ATP/ADP-cycle-catalyzing ribozyme is present at this stage, but the turnover rate of the ATP/ADP cycle is tripled. The allosterase R_5undergoes ATP-induced conversion to its allosteric counterpart R_6, which subsequently catalyzes the conversion of parasitic ribozymes R_3 into the allostery-prone forms R_7 and R_8. Under these conditions, complete stabilization is achieved. **b-g** Evolution of R_1, R_3, R_5, R_6, R_7, and R_8, respectively. (D_—), (D_tot – –), (delta_—), (T_—), (T_tot– –); (R_1, blue; total $R_{1,\mathrm{tot}}$, brown; R_3, blue; total $R_{3,\mathrm{tot}}$, brown; R_5, blue; total $R_{5,\mathrm{tot}}$, brown; R_6, blue; total $R_{6,\mathrm{tot}}$, brown; R_7, blue; total $R_{7,\mathrm{tot}}$, brown; R_8, blue; total $R_{8,\mathrm{tot}}$, brown).

Fig. 8. Parasite ribozymes R_3evolve into ATPase/ATP synthetase ribozymes

a Evolution of ADP (D_), ATP (T_), and (delta_); ATPase/ATP synthase activity has emerged from the parasitic ribozyme R_3 **c**. As shown in Fig. 4, ATP-dependent allosteric regulation by R_4**d** tames parasitism by R_3, but requires additional ATP turnover that is supplied by the newly evolved ATPase/ATP synthase activity. **b-d** Evolution of R_1, R_3, and R_4, respectively. (D_—), (D_tot – –), (delta_—), (T_—), (T_tot– –); (R_1, blue; total $R_{1,\mathrm{tot}}$, brown; R_3, blue; total $R_{3,\mathrm{tot}}$, brown, R_4, blue; total $R_{4,\mathrm{tot}}$, brown).

Fig. 9. ATPase/ATP synthase ribozymes enable resistance to subsequent parasite invasion

a Evolution of ADP (D_), ATP (T_), and (delta_); ATPase/ATP synthase activity has emerged from the parasitic ribozyme R_3 **c**. The resulting allosterically regulated habitat **d**, supported by sufficient ATP supply **a**, resists subsequent invasion by parasitic ribozymes R_5 and R_6 **e-f**, provided that newly emerging parasites are allostery-prone. **b-f** Evolution of R_1, R_3, R_4, R_5, and R_6, respectively. (D_—), (D_tot – –), (delta_—), (T_—), (T_tot– –); (R_1,

blue; total $R_{1,\mathrm{tot}}$, brown; R_3, blue; total $R_{3,\mathrm{tot}}$, brown, R_4, blue; total $R_{4,\mathrm{tot}}$, brown, R_5, blue; total $R_{5,\mathrm{tot}}$, brown, R_6, blue; total $R_{6,\mathrm{tot}}$, brown).

Fig. 10. Habitat with ATPase/ATP synthetase ribozymes and allosterases recapitulates parasite resistance

a Evolution of ADP (D_), ATP (T_), and (delta_); ATPase/ATP synthase activity emerges from the parasitic ribozyme R_3 **c.** The resulting integrated system, comprising the host replicase R_1 **b**, the ATP synthase/ATPase ribozyme R_3 and its allosteric counterpart R_4 **c-d**, and the allosterase pair R_5 and R_6 **e-f**, remains stable following the emergence of the non-allostery-prone parasitic ribozyme R_7 **g**. The allosterase subsequently converts R_7 into the allostery-prone forms R_9 and R_{10} **h-i**, thereby maintaining parasite resistance. (D_—), (D_tot – –), (delta_—), (T_—), (T_tot– –); (R_1, blue; total $R_{1,\mathrm{tot}}$, brown; R_3, blue; total $R_{3,\mathrm{tot}}$, brown, R_4, blue; total $R_{4,\mathrm{tot}}$, brown, R_5, blue; total $R_{5,\mathrm{tot}}$, brown, R_6, blue; total $R_{6,\mathrm{tot}}$, brown, R_7, blue; total $R_{7,\mathrm{tot}}$, brown, R_9, blue; total $R_{9,\mathrm{tot}}$, brown, R_{10}, blue; total $R_{10,\mathrm{tot}}$, brown).

Supplementary Files

This is a list of supplementary files associated with this preprint. Click to download.

- SupplementaryinformationConradetal.171026.docx